International Journal of Applied Pharmaceutics

ISSN- 0975-7058 Vol 13, Special Issue 4, 2021

Original Article

MOLECULAR DOCKING AND MOLECULAR DYNAMICS STUDIES OF *ACALYPHA INDICA* L. PHYTOCHEMICAL CONSTITUENTS WITH CASPASE-3

ELLIN FEBRINA[1,2*], RYAN KHUNAM ALAMHARI[3], AIYI ASNAWI[3], RIZKY ABDULAH[2], KERI LESTARI[2,4], JUTTI LEVITA[2], UNANG SUPRATMAN[1,5]

[1]Department of Chemistry, Faculty of Mathematics and Natural Sciences, [2]Department of Pharmacology and Clinical Pharmacy, Faculty of Pharmacy, Universitas Padjadjaran, Jl. Raya Bandung-Sumedang km. 21, Jatinangor, 45363, Indonesia, [3]Department of Pharmacochemistry, Faculty of Pharmacy, Universitas Bhakti Kencana, Jl. Soekarno-Hatta No. 754, Bandung, 40617, Indonesia, [4]Center of Excelence in Higher Education for Pharmaceutical Care Innovation, Universitas Padjadjaran, Jl. Dipatiukur No. 35, Bandung, 40132, Indonesia, [5]Central Laboratory, Universitas Padjadjaran, Jl. Raya Bandung-Sumedang km. 21, Jatinangor, 45363, Indonesia
[*]Email: ellin.febrina@unpad.ac.id

Received: 20 Aug 2021, Revised and Accepted: 05 Oct 2021

ABSTRACT

Objective: This study investigated the structure-based molecular interactions between phytochemical constituents of *Acalypha indica* L. and caspase-3.

Methods: Thirty-three phytochemical constituents of *A. indica* were screened against caspase-3. The X-ray crystal structure of human caspase-3 was retrieved from https://www.rcsb.org/structure/. The molecular interactions of the phytochemicals were studied using the AutoDock 4.2 software and followed by molecular dynamics (MD) simulations using the Amber18 software.

Results: From this study, 25 screened phytochemicals were found to have a better binding mode than the native ligand. Moreover, the binding stability of the top four hits evaluated by MD indicated that the hydrogen bonds in MD were quite different from the molecular docking results due to the massive receptor and ligand movement in the MD simulations. However, with the exception of stigmasterol, all ligands were able to stabilize the protein.

Conclusion: This study suggested that γ-sitosterol acetate, β-sitosterol acetate, and γ-sitosterol might be able to induce caspase-3, thereby activating apoptosis. These high-affinity compounds can bind to caspase-3 more efficiently and were able to stabilize the protein. Therefore, they have the potential to be used as lead compounds in the treatment of cancer.

Keywords: *Acalypha indica* L., Apoptosis, Caspase-3, Molecular docking, Molecular dynamics

© 2021 The Authors. Published by Innovare Academic Sciences Pvt Ltd. This is an open access article under the CC BY license (https://creativecommons.org/licenses/by/4.0/)
DOI: https://dx.doi.org/10.22159/ijap.2021.v13s4.43861 Journal homepage: https://innovareacademics.in/journals/index.php/ijap

INTRODUCTION

Acalypha indica L. is a medicinal plant that has been known as a source of traditional medicine for treating several diseases in ethnomedicinal practices [1-10]. The *A. indica* extracts have been reported to possess many pharmacological activities, such as anti-arthritis, antibacterial, antidiabetic, antifungal, antihyperlipidemic, anti-inflammatory, and others [6, 9, 11-14]. Previous studies have also shown that *A. indica* extracts have potential antiproliferative activity in several cancer cell lines, including PC3 prostate cancer, HT-29 colon cancer, and NCI-H187 small cell lung cancer [15-17]. Furthermore, scientists have identified the phytochemical constituents of this plant which are included in the secondary metabolites of alkaloids, flavonoids, phenolics, tannins, and steroids [1, 18-20]**.** Although *A. indica* has been reported to inhibit several types of cancer growth and has many phytochemicals, until now, progress in the discovery of anticancer lead compounds from this plant is still limited.

The computational method has been regarded as a simple and cost-effective way of discovering compounds with high biological activity for drug development. It gives a thorough assessment of the relevant characteristics and interactions of compounds, minimizing mistakes and undesired findings during *in vitro* studies [21]. One of the targets of anticancer drugs is apoptosis (programmed cell death) [22]. Caspases play an important role in the regulation of apoptosis [22]. While caspase-3 is an essential component in some apoptosis pathways [23]. This study aimed to investigated the structure-based molecular interactions between the phytochemical constituents of *A. indica* and caspase-3.

MATERIALS AND METHODS

Hardware and software

The hardware used in this study was a computer unit equipped with an Intel® Core™ i7-7200U CPU @2.50 GHz (4 CPUs. 2.7 GHz), 8 GB of RAM, and a dual-boot OS: Windows 10 Pro 64-bit operating system, ×64-based processor, and Linux Ubuntu 16.04 LTS 64-bit. Visualization of docking poses and interacting were carried out by using the Discovery Studio Visualizer [24]. Preparation of macromolecule and ligands, as well as docking studies, were carried out using AutoDock 4.2 [25-27] and exploring ligand stability in protein crystal structures was carried out using Amber18 [28].

Macromolecule preparation

The crystal structure of caspase-3 was taken from the Protein Data Bank with PDB ID 1NME [29, 30]. The small molecules and water molecules in the macromolecule were removed, and polar hydrogens and Kollman charges were added.

Ligand preparation

The three-dimensional structures of the 33 phytochemical constituents of *A. indica* (ligands) were retrieved from the PubMed structure database and 2-Hydroxy-5-(2-mercapto-ethyl sulfa-moyl)-benzoic acid (PDB ID 159) is the native ligand (NL) for caspase-3 (PDB ID 1NME).

Molecular docking studies

Preparation of caspase-3 macromolecular coordinates and ligands, including polar hydrogen atoms, was carried out using AutoDock Tools 1.5.6. Pre-calculation of atomic affinities was performed using AutoGrid. A grid box comprised of 40 × 40 × 40 points with a spacing of 0.375 Å and was focused on the dimensions of 101.360 × 87.332 × 31.445 points. The Lamarckian Genetic Algorithm (LGA) and specifications were 100 runs, elitism of 1, the mutation rate of 0.02, the population size of 100, a crossover rate of 0.08, and 2.500.000 energy evaluations. The docking results were visualized using the Discovery Studio Visualizer 3.5 package [24].

MD studies

Ligands with top hits scores were selected for further MD studies. MD simulations were performed with the Amber18 software. The

Amber ff14SB force field was applied to caspase-3 macromolecule, and charges were added to the macromolecules using the software's database. The general AMBER force field (GAFF2) was applied to the structures with the top hit score and NL, and the AM1-BCC method was taken to determine its partial charge in the GAFF2 force field [31]. The ligand topology and atomic charge files were generated by applying the Antechamber suite. The root mean squared deviation (RMSD), root mean squared fluctuation (RMSF), and the interaction energy of all protein-ligand complexes was used to assess the stability of the system after 100 ns of MD simulation.

RESULTS

In this study, 33 phytochemical constituents of *A. indica,* collected from the reference [1], were docked onto the active site of the caspase-3 macromolecular target and their binding affinities were evaluated (table 1). The RMSD value of the overlay of the docked pose and the X-ray crystal structure of the NL was 1.34 Å. The binding energy and inhibitory constant of the NL were-4.28 kcal/mol and 724.43 μM, respectively. The binding mode of NL showed hydrogen bond interactions with the amino acid residues of Arg64, Gly122, Cys163, Gln161, Ser205, and Arg207 (fig. 1A).

Table 1: Binding affinity of the protein-ligand interaction of phytochemical constituents of *Acalypha indica* L.

Entry	Ligand	Binding affinity (kcal/mol)	Ki (μM)	Protein-ligands interaction	
				No. of H bonds	Amino acid involved in interaction
NL	2-Hydroxy-5-(2-mer-captoethylsulfamoyl)-benzoic acid (ID: 159)	-4.28	724.43	8	Arg64, Gly122, Cys163, Gln161, Ser205, Arg207
1	γ-Sitosterol acetate	-8.08	1.20	2	Asn208, Trp214
2	β-Sitosterol acetate	-8.02	1.33	1	Glu248
3	Stigmasterol	-7.70	2.27	0	-
4	γ-Sitosterol	-7.41	3.71	0	-
5	Naringin	-6.97	7.74	6	Tyr204, Arg207, Glu248, Phe250, Phe252
6	Geranin	-6.92	8.54	5	Tyr204, Arg207, Ser209, Trp214, Glu248
7	β-Sitosterol ß-D-glucoside	-6.59	14.83	2	Glu248, Ser249
8	Naringenin	-6.48	17.73	4	Trp214, Glu248, Phe250, Ser251
9	Acaindinin	-6.39	20.59	9	Arg207, Asn208, Trp214, Glu248, Phe250, Ser251, Phe252
10	Kaempferol	-6.19	28.90	5	Arg207, Trp214, Glu248, Phe250, Ser251
11	Hesperetin	-6.16	30.34	5	Asn208, Trp214, Glu248, Ser251, Phe252
12	Chrysin	-6.08	34.72	3	Trp214, Glu248, Phe250
13	Galangin	-6.03	38.07	4	Arg207, Trp214, Glu248, Phe250
14	Tectoquinone	-5.96	42.53	2	Trp214, Phe250
15	2-Methyl anthraquinone	-5.96	42.45	2	Trp214, Phe250
16	Quinine	-5.88	48.75	2	Trp214, Phe250
17	Nicotiflorin	-5.82	54.50	9	Arg207, Asn208, Trp214, Glu248, Phe250, Ser251
18	Quercetin	-5.76	60.20	5	Arg297, Trp214, Glu248, Phe250, Ser251
19	Tri-O-methylellagic acid	-5.63	74.55	4	Asn208, Ser209, Phe250
20	4,4′,5,5′,6,6′-Hexahydroxy diphenic acid	-5.38	113.93	4	Ser205, Arg207, Glu248, Phe250
21	Corilagin	-5.36	117.33	7	Tyr204, Ser209, Trp214, Glu248, Phe252
22	Glucogallin	-5.45	100.92	9	Arg207, Ser209, Trp214, Glu248, Phe50
23	Ellagic acid	-5.32	126.52	4	Arg207, Ser209, Glu248, Phe250
24	4-Amino-3-methoxypyrazolo[3,4-d] pyrimidine	-4.60	426.35	3	Arg207, Glu248, Phe250
25	Acalyphin amide	-4.55	461.83	9	Asn208, Ser209, Trp214, Glu248, Phe250
26	1,3-Dioxolane, 4-Ethyl-5-Octyl-2,2-Bis (Trifluoromethyl)-, Trans-	-4.15	902.45	2	Phe250, Asn208
27	Syringic acid	-4.12	958.61	3	Ser209, Phe250
28	Caffeic acid	-4.07	1.03	3	Ser209, Glu248
29	Gallic acid	-3.97	1.24	6	Arg207, Ser209, Phe250
30	Ferulic acid	-3.94	1.29	4	Tyr204, Phe250, Phe252
31	3,8-Nonadien-2-one, E	-3.82	1.59	1	Asn208
32	Quebrachitol	-3.78	1.70	3	Trp214, Glu248, Phe250
33	Catechol	-3.64	2160.00	2	Phe250

Based on molecular docking, binding affinity, inhibitory constant, number of hydrogen bonds in the binding site, and interactions between 33 ligands and proteins at the binding site were predicted (table 1). The results showed that almost all the ligands have similar orientations in the binding pocket of the caspase-3 crystal structure with a binding energy range of-3.64 to-8.08 kcal/mol. The 25 screened phytochemicals were found to have a better binding mode than the NL. The top four hits based on binding energy were compounds 1, 2, 3, and 4 with binding energies of-8.08,-8.02,-7.70, and-7.41 kcal/mol, respectively. Compound 1 showed two hydrogen bonds with Asn208 and Trp214 residues and compound 2 showed one hydrogen bond with Glu248 residue (fig. 1B-C). Both of these compounds formed no pi sigma-interaction. Compounds 3 and 4 formed no hydrogen bonds and one pi sigma-interaction with Phe250 and Phe252 residues, respectively (fig. 1D-E).

The MD simulation was carried out to determine the stability of the protein-ligand complex. The binding stability studies on the top four ligands 1, 2, 3, and 4 with the highest affinity for caspase-3 showed the RMSD values of backbone atoms on the ligands (fig. 2). Residual fluctuation behavior studies showed that, in general, the RMSF value of each residue in the ligand complex was less than 2 Å. However, it can also be observed that there was the instability of Asp146 residue in the caspase-3 complex with all compounds shown with RMSF values of 8.28 (fig. 3). The fluctuation behavior of NL into the binding site of caspase-3 revealed four hydrogen bonds with the backbones of Arg64, Cys163, Ser205, and Arg207 with RMSF of 2.81, 2.74, 3.05, and 2.78 Å, respectively, while the compounds 1, 2, 3, and 4 interacted with the side chain of Trp214 and Phe252 (table 2). The binding free energies of the complexes of caspase-3 with NL or the compounds 1, 2, 3, and 4 were-45.0359,-52.0814,-37.7693,-23.7661, and-16.2200 kcal/mol, respectively (table 3).

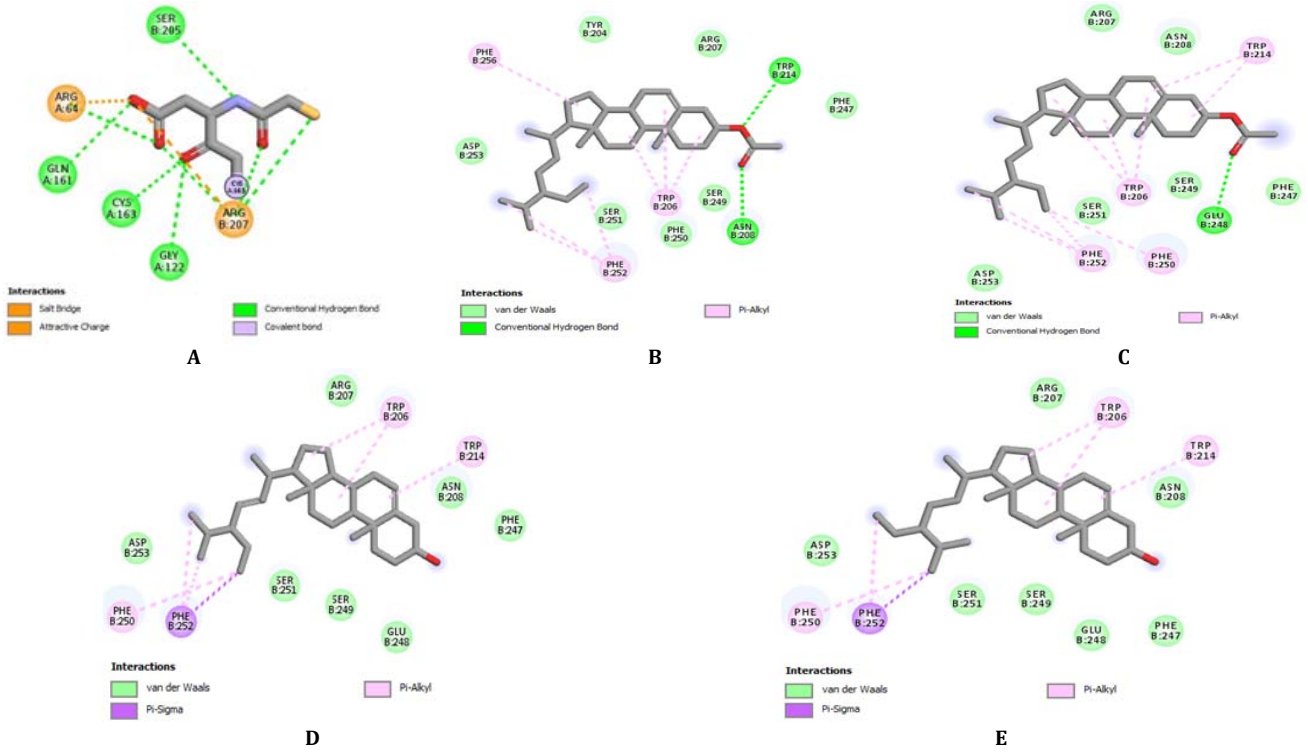

Fig. 1: Amino acid interaction of caspase-3 protein complexes with [A] native ligand (NL), [B] γ-sitosterol acetate (1), [C] β-sitosterol acetate (2), [D] stigmasterol (3), [E] γ-sitosterol (4)

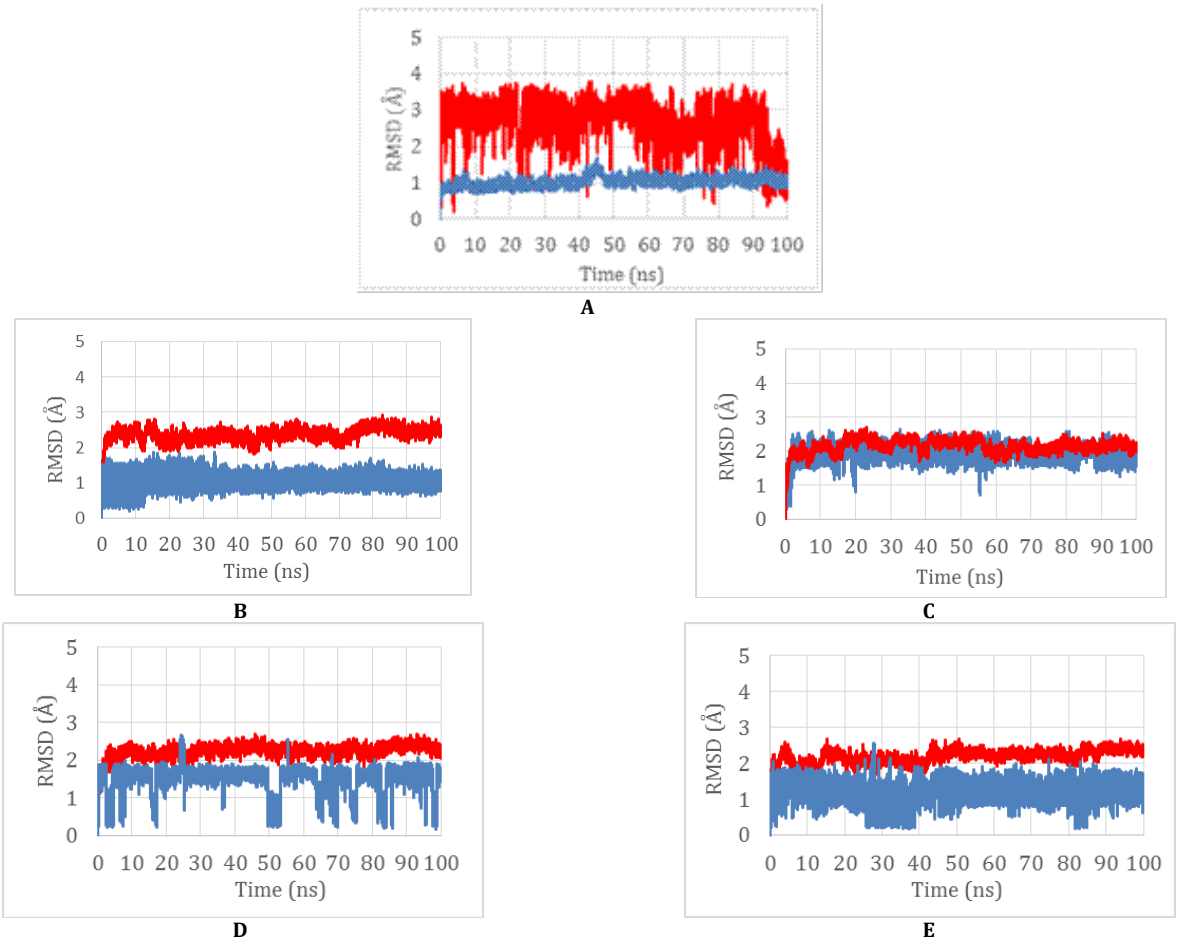

Fig. 2: RMSD backbone atoms on [A] native ligand (NL), [B] γ-sitosterol acetate (1), [C] β-sitosterol acetate (2), [D] stigmasterol (3), [E] γ-sitosterol (4) for 100 ns MD simulation with caspase-3 macromolecule (red: protein structure and blue: ligand)

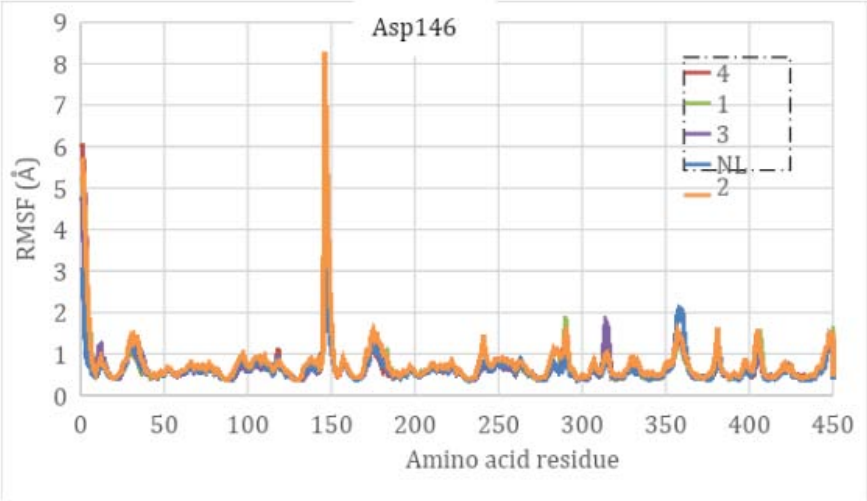

Fig. 3: RMSF of backbone and side-chain atoms versus residue numbers of all compounds

Table 2: Fluctuation behavior of residues into the binding site

Residue	RMSF for individual amino acid residue (Å)				
	NL	1	2	3	4
Arg64	2.81				
Cys163	2.74				
Ser205	3.05				
Arg207	2.78				
Trp214		3.15	4.75	4.71	4.76
Phe252		4.01	3.45	4.51	3.4

Table 3: The binding free energy (ΔG_{bind}) component of the complex proteins with compounds

Energies (kcal/mol)	The binding free energy (ΔG_{bind}) component of the complex of proteins with compounds				
	NL	1	2	3	4
ΔE_{vdw}	-18.6234	-21.6329	-20.1085	-14.8235	-23.3539
ΔE_{ele}	-14.7677	-4.4078	-1.8163	-0.8100	-1.2847
ΔG_{p}	21.7463		6.0802	7.5008	8.4223
ΔG_{np}	-33.3911	-26.0407	-21.9247	-15.6334	-24.6385
ΔG_{bind}	-45.0359	-52.0814	-37.7693	-23.7661	-16.2200

DISCUSSION

The binding affinity between the 33 ligands and the crystal structure of caspase-3 was predicted by the scoring function. RMSD parameters were used to verify the position of the binding site for the NL, which was performed by overlaying the docked pose and the X-ray crystal structure of the NL. The RMSD value of 1.34 Å indicates that the docking process can reproduce the correct binding pose of the NL ligand to its receptor. The binding mode of NL with caspase-3 macromolecules is quite similar to that which has been reported by Erlanson, *et al.*, 2003 [29].

Molecular docking results showed that compound 4, as well as compound 1, is an epimer of β-sitosterol and compound 2, respectively. Compounds 1 and 2, which have the same substituent but different conformation, have different free energy of binding and number of hydrogen bonds (2:1) and hydrophobic (7:9). Compound 4, which has no substituent, has a lower free energy of binding and a different number of hydrogen bonds (0) and hydrophobic (6) compared to compounds 1 and 2. This indicates that the acetate substituent plays an important role in the formation of hydrogen bonds in the three sitosterol compounds. Compound 4 has potential anti-cancer activity through growth inhibition, cell cycle arrest, and apoptosis in breast and lung cancer cells [32], and is cytotoxic against colon and liver cancer cells [33]. It is necessary to conduct MD simulations for compounds 1, 2, 3, and 4 to investigate the stability of the protein-ligand interactions.

MD simulations with the molecular mechanics generalized Born surface area (MM/GBSA) methods were used to investigate the interaction dynamics between ligands 1, 2, 3, 4 and their targets. The goal of these simulations was to investigate the impact of ligand binding on the residues of protein targets, particularly at the binding areas. Strong binders tend to reduce the mobility of the atoms they bind to and, as a result, stabilize the protein's binding area. This was investigated by determining the RMSD of the protein binding site atoms throughout the course of a 100 ns simulation. Furthermore, the RMSF was used to calculate the total fluctuation of each atom in the binding site relative to the reference structure.

The complex of caspase-3 with NL showed stability at 10-100 ns, although there was a small movement with an RMSD value of less than 2 Å. The complex of caspase-3 with ligands 1 and 4 achieved stability from the start of 0 ns with an average RMSD value of 1.104 Å. Meanwhile, the complex of caspase-3 with ligand 2 starts to reach stability around 5-100 ns, but at 5 ns it is suspected that the ligand has moved from its initial position as indicated by an RMSD value of more than 2.5 Å. The stability of this complex begins to be achieved after 5 ns at a new position.

Moreover, the complex of caspase-3 with ligand 3 had an average RMSD value of 2.233 Å. This ligand did not achieve stability and was likely to escape from the receptor at 25 ns, as indicated by its RMSD value of more than 2 Å. After the test time was added, the possibility of re-release occurred at around 55 ns and no stable interaction occurred. All ligands

were able to stabilize the receptor as seen from the average RMSD of the receptor of 2.317 Å. The receptor that binds to NL have an average RMSD of 2.657 Å due to the very complex structure of the receptor with a very large number of atoms, so that the slightest movement of atoms from the receptor will cause the RMSD value to change greatly.

RMSF was used to explore the stability of the residue at the binding site during the 100 ns simulation. The RMSF of all residues around the ligands was counted in the last 40 ns pass by using the Discovery Studio. The complex as a result of the simulation is calculated through visualization and transformation in the mean structure (fig. 3). The RMSF of each residue in the complex was less than 2 Å, which indicates that the binding site was quite stable during the simulation [34]. The instability of Asp146 residues in the caspase-3 complexes with all compounds were possible because the position of the Asp146 residue is not at the side chain binding site but at the end of the protein structure.

The binding free energies (ΔG_{bind}) of the complexes of caspase-3 with NL or the compounds 1, 2, 3, and 4 consist of the van der Waals interaction energy (ΔE_{vdw}), the electrostatic interaction energy (ΔE_{ele}), the polar solvation free energy (ΔG_p), and the non-polar solvation free energy (ΔG_{np}). It can be concluded that van der Waals provides the main driving force for the complexes of caspase-3 with compounds 1, 2, and NL. However, the polar and non-polar solvation energies are unfavorable for the binding free energies. The binding stability of the top four hits evaluated by MD simulations indicated that the hydrogen bonds in MD were quite different from the molecular docking results due to the massive receptor and ligand movement in the MD simulations.

CONCLUSION

This study suggested that γ-sitosterol acetate, β-sitosterol acetate, and γ-sitosterol might be able to induce caspase-3 thereby activate apoptosis. These high-affinity compounds can bind to caspase-3 more efficiently and were able to stabilize the protein. Therefore, they have the potential to be used as lead compounds in the treatment of cancer.

ACKNOWLEDGEMENT

The present study is part of a dissertation research that was financially supported by the Indonesia Endowment Fund for Education through the Indonesian Education Scholarship for Doctoral Program, 2016-2020 for EF.

AUTHORS CONTRIBUTIONS

All the authors have equally contributed to the current study.

CONFLICT OF INTERESTS

The authors declare no conflicts of interest.

REFERENCES

1. Zahidin NS, Saidin S, Zulkifli RM, Muhamad II, Ya'akob H, Nur H. A review of Acalypha indica L. (Euphorbiaceae) as traditional medicinal plant and its therapeutic potential. J Ethnopharmacol. 2017;207:146-73. doi: 10.1016/j.jep.2017.06.019, PMID 28647509.
2. Savithramma N, Sulochana Ch, Rao KN. Ethnobotanical survey of plants used to treat asthma in Andhra Pradesh, India. J Ethnopharmacol. 2007;113(1):54-61. doi: 10.1016/ j.jep.2007.04.004, PMID 17606346.
3. Das PR, Akter S, Islam MT, Kabir MH, Haque MM, Khatun Z. A selection of medicinal plants used for treatment of diarrhea by folk medicinal practitioners of Bangladesh. Am–Eurasia J Sustain Agric. 2012;6:153-61.
4. Mohan C, Dinakar S, Anand T, Elayaraja R, Sathiya Priya B. Phytochemical, GC-MS analysis and antibacterial activity of a medicinal plant Acalypha indica. Int J Pharm Tech Res. 2012;4:1050-4.
5. Divya N, Thenmozhi S, Sureshkumar B, Selvan M. Antibacterial activity of medicinal plant against wound infected pathogens. Int J Pharm Sci Res. 2014;5:4942-7.
6. Saha R, Ahmed A. Phytochemical constituents and pharmacological activities of Acalyphus indica Linn: a review. Int J Pharm Sci Res. 2011;2:1900-4.
7. Ribeiro A, Romeiras MM, Tavares J, Faria MT. Ethnobotanical survey in Canhane village, district of Massingir, Mozambique: medicinal plants and traditional knowledge. J Ethnobiol Ethnomed. 2010;6:33. doi: 10.1186/1746-4269-6-33, PMID 21129187.
8. Singh AG, Kumar A, Tewari DD. An ethnobotanical survey of medicinal plants used in Terai forest of western Nepal. J Ethnobiol Ethnomed. 2012;8:19. doi: 10.1186/1746-4269-8-19, PMID 22591592.
9. Jayaprakasam R, Ravi T. Evaluation of anti-arthritic activity of the root extract of Acalypha indica Linn. using *in vitro* techniques. Int J Phytopharmacol. 2013;2:169-73.
10. Marwah RG, Fatope MO, Al Mahrooqi R, Varma GB, Al Abadi H. Al-Burtamani. SKS. Antioxidant capacity of some edible and wound healing plants in Oman. Food Chem 2007;101:465-70.
11. Govindarajan M, Jebanesan A, Reetha D, Amsath R, Pushpanathan T, Samidurai K. Antibacterial activity of Acalypha indica L. Eur Rev Med Pharmacol Sci. 2008;12(5):299-302. PMID 19024213.
12. Solomon RDJ, Kallidass S, Vimalan J. Isolation, identification and study of antimicrobial property of a bioactive compound in an Indian medicinal plant Acalypha indica (Indian-nettle). World J Microbiol Biotechnol. 2005;21(6-7):1231-6. doi: 10.1007/s11274-005-1479-6.
13. Rajasekaran S, Anandan R, Nishad K. Antihyperlipidemic activity of Acalypha indica Linn. on atherogenic diet induced hyperlipidemia. Int J Pharm Pharm Sci. 2013;5:699-701.
14. Rahman MA, Bachar SC, Rahmatullah M. Analgesic and antiinflammatory activity of methanolic extract of Acalypha indica Linn. Pak J Pharm Sci. 2010;23(3):256-8. PMID 20566436.
15. Amarnath K, Dhanabal J, Agarwal I, Seshadry S. Cytotoxicity induction by ethanolic extract of Acalypha indica loaded casein-chitosan microparticles in human prostate cancer cell line *in vitro*. Biomed Prev Nutr. 2014;4(3):445-50. doi: 10.1016/j.bionut.2013.03.009.
16. Nagendran S, Muthukumar T, Ramalingam S, Palanisamy S, Hameed SS. Influence of Acalypha indica in cell proliferation, cell cycle arrest and anticancer activity in HT-29 colon cell lines. Pharm Lett. 2015;7(9):40-52.
17. Sanseera D, Niwatananun W, Liawruangrath B. Antioxidant and anticancer activities from aerial parts of Acalypha indica Linn. Chiang Mai Univ J Nat Sci. 2012;11(2):157-68.
18. Ma YT, Chuang JI, Lin JH, Hsu F. Phenolics from acalypha indica. Int Chinese Chemical Soc. 1997;44(5):499-502. doi: 10.1002/jccs.199700075.
19. Nahrstedt A, Hungeling M, Petereit F. Flavonoids from Acalypha indica. Fitoterapia. 2006;77(6):484-6. doi: 10.1016/j.fitote.2006.04.007, PMID 16828241.
20. Ghani A. Medicinal plants of Bangladesh: chemical constituents and uses. 2nd ed. Dhaka: Asiatic Society of Bangladesh; 2003.
21. Balakrishnan NA, Raj JS, Kandakatla NA. *In silico* studies on new indazole derivatives as GSK-3 inhibitors. Int J Pharm Pharm Sci. 2015;7:295-9.
22. Porter AG, Jänicke RU. Emerging roles of caspase-3 in apoptosis. Cell Death Differ. 1999;6(2):99-104. doi: 10.1038/sj.cdd.4400476, PMID 10200555.
23. McIlwain DR, Berger T, Mak TW. Caspase functions in cell death and disease. Cold Spring Harb Perspect Biol. 2013;5(4):a008656. doi: 10.1101/cshperspect.a008656, PMID 23545416.
24. Visualizer. ADS Version 4. 5. Softw. Vis. Anal. Protein Struct.; 2017.
25. Rizvi SMD, Shakil S, Haneef M. A simple click by click protocol to perform docking: AutoDock 4.2 made easy for non-bioinformaticians. Excli J. 2013;12:831-57. PMID 26648810.
26. Muttaqin FZ, Kharisma D, Asnawi A, Kurniawan F. Pharmacophore and molecular docking-based virtual screening of B-cell lymphoma 2 (BCL 2) inhibitor from zinc natural database as anti-small cell lung cancer. J Drug Delivery Ther. 2020;10(2):143-7. doi: 10.22270/jddt.v10i2.3923.
27. Nursamsiar N, Mangande M, Awaluddin A, Nur S, Asnawi A. *In silico* study of aglycon curculigoside A and its derivatives as α-

amilase inhibitors. Indonesian J Pharm Sci Technol. 2020;7(1):29-37. doi: 10.24198/ijpst.v7i1.23062.

28. Lee TS, Cerutti DS, Mermelstein D, Lin C, LeGrand S, Giese TJ, Roitberg A, Case DA, Walker RC, York DM. GPU-accelerated molecular dynamics and free energy methods in Amber18: performance enhancements and new features. J Chem Inf Model. 2018;58(10):2043-50. doi: 10.1021/acs.jcim.8b00462, PMID 30199633.
29. Erlanson DA, Lam JW, Wiesmann C, Luong TN, Simmons RL, DeLano WL, Choong IC, Burdett MT, Flanagan WM, Lee D, Gordon EM, O'Brien T. *In situ* assembly of enzyme inhibitors using extended tethering. Nat Biotechnol. 2003;21(3):308-14. doi: 10.1038/nbt786, PMID 12563278.
30. Megantara S, Mutakin M, Halimah E, Febrina E, Levita J. Molecular interaction of the downstream executioner cysteine aspartyl proteases (caspase-3 and caspase-7) with corilagin, quercetin, rutin, kaempferol, gallic acid, and geraniin of Acalypha wilkesiana mull. Arg Rasayan J Chem. 2020;13(3):1321-9. doi: 10.31788/RJC.2020.1335766.
31. Jakalian A, Bush BL, Jack DB, Bayly CI. Fast, efficient generation of high-quality atomic charges. AM1-BCC model: I. Method. J Comput Chem. 2000;21(2):132-46. doi: 10.1002/(SICI)1096-987X(20000130)21:2<132:AID-JCC5>3.0.CO;2-P.
32. Sundarraj S, Thangam R, Sreevani V, Kaveri K, Gunasekaran P, Achiraman S, Kannan S. γ-sitosterol from Acacia nilotica L. induces G2/M cell cycle arrest and apoptosis through c-Myc suppression in MCF-7 and A549 cells. J Ethnopharmacol. 2012;141(3):803-9. doi: 10.1016/j.jep.2012.03.014, PMID 22440953.
33. Endrini S, Rahmat A, Ismail P, Taufiq Yap YH. Cytotoxic effect of γ-sitosterol from Kejibeling (Strobilanthes crispus) and its mechanism of action towards c-myc gene expression and apoptotic pathway. Med J Indones. 2014;23(4):203-8. doi: 10.13181/mji.v23i4.1085.
34. Cole JC, Murray CW, Nissink JWM, Taylor RD, Taylor R. Comparing protein-ligand docking programs is difficult. Proteins. 2005;60(3):325-32. doi: 10.1002/prot.20497, PMID 15937897.